Characterisation of retinoblastomas without *RB1* mutations: genomic, gene expression, and clinical studies

Diane E Rushlow, Berber M Mol, Jennifer Y Kennett,* Stephanie Yee,* Sanja Pajovic, Brigitte L Thériault, Nadia L Prigoda-Lee, Clarellen Spencer, Helen Dimaras, Timothy W Corson, Renée Pang, Christine Massey, Roseline Godbout, Zhe Jiang, Eldad Zacksenhaus, Katherine Paton, Annette C Moll, Claude Houdayer, Anthony Raizis, William Halliday, Wan L Lam, Paul C Boutros, Dietmar Lohmann, Josephine C Dorsman, Brenda L Gallie*

Summary

Background Retinoblastoma is the childhood retinal cancer that defined tumour-suppressor genes. Previous work shows that mutation of both alleles of the *RB1* retinoblastoma suppressor gene initiates disease. We aimed to characterise non-familial retinoblastoma tumours with no detectable *RB1* mutations.

Methods Of 1068 unilateral non-familial retinoblastoma tumours, we compared those with no evidence of *RB1* mutations ($RB1^{+/+}$) with tumours carrying a mutation in both alleles ($RB1^{-/-}$). We analysed genomic copy number, *RB1* gene expression and protein function, retinal gene expression, histological features, and clinical data.

Findings No *RB1* mutations ($RB1^{+/+}$) were reported in 29 (2·7%) of 1068 unilateral retinoblastoma tumours. 15 of the 29 $RB1^{+/+}$ tumours had high-level *MYCN* oncogene amplification (28–121 copies; $RB1^{+/+}MYCN^{A}$), whereas none of 93 $RB1^{-/-}$ primary tumours tested showed *MYCN* amplification (p<0·0001). $RB1^{+/+}MYCN^{A}$ tumours expressed functional RB1 protein, had fewer overall genomic copy-number changes in genes characteristic of retinoblastoma than did $RB1^{-/-}$ tumours, and showed distinct aggressive histological features. *MYCN* amplification was the sole copy-number change in one $RB1^{+/+}MYCN^{A}$ retinoblastoma. One additional $MYCN^{A}$ tumour was discovered after the initial frequencies were determined, and this is included in further analyses. Median age at diagnosis of the 17 children with $RB1^{+/+}MYCN^{A}$ tumours was 4·5 months (IQR 3·5–10), compared with 24 months (15–37) for 79 children with non-familial unilateral $RB1^{-/-}$ retinoblastoma.

Interpretation Amplification of the *MYCN* oncogene might initiate retinoblastoma in the presence of non-mutated *RB1* genes. These unilateral $RB1^{+/+}MYCN^{A}$ retinoblastomas are characterised by distinct histological features, only a few of the genomic copy-number changes that are characteristic of retinoblastoma, and very early age of diagnosis.

Funding National Cancer Institute–National Institutes of Health, Canadian Institutes of Health Research, German Research Foundation, Canadian Retinoblastoma Society, Hyland Foundation, Toronto Netralaya and Doctors Lions Clubs, Ontario Ministry of Health and Long Term Care, UK-Essen, and Foundations Avanti-STR and KiKa.

Introduction

Retinoblastoma set the paradigm for tumour-suppressor genes, with Knudson's classic hypothesis predicting that two rate-limiting hits initiate this childhood eye cancer.[1] The two hits were later attributed to the retinoblastoma gene (*RB1*).[2] 40% of children with retinoblastoma have bilateral disease. They carry a constitutional *RB1* mutation that predisposes to retinoblastoma; one additional hit damages the second *RB1* allele and initiates retinoblastoma or other cancers later in life. In 70% of bilateral tumours, the second hit entails loss of the normal allele with duplication of the mutant allele (loss of heterozygosity). The other 60% of children with retinoblastoma have unilateral non-familial disease. In these cases, usually both *RB1* alleles are damaged only in the developing retina, but 15% carry a heritable constitutional *RB1* mutation. Accepted dogma is that disruption of both *RB1* alleles ($RB1^{-/-}$) initiates all cases of retinoblastoma.[2–4]

The mutant *RB1* allele is identifiable in blood samples of 95% of bilaterally affected patients. Low-level mosaicism can account for the remaining 5% of blood samples in which no mutation is found.[5] Previously, we have identified mutations in both *RB1* alleles (or promoter methylation) in more than 95% of tumours from unilateral probands with no known family history.[5,6] In 3–4% of tumours, we identified only one *RB1* mutation, and in 2% we saw no disruption to *RB1*. Undetected *RB1* mutations in fully tested tumours ($RB1^{+/+}$) might include translocations, deep intronic mutations, or alterations in unknown *RB1* regulatory regions. The possibility that some unilateral retinoblastomas with no detectable *RB1* mutations arise by an independent mechanism has, to our knowledge, not been investigated before. We aimed to characterise unilateral retinoblastomas with non-mutated *RB1* alleles for other genetic changes.

Methods

Study population

Five clinical laboratories took part in this study: Impact Genetics (formerly Retinoblastoma Solutions), Toronto, Canada; Institut für Humangenetik, Essen, Germany;

Lancet Oncol 2013; 14: 327–34

Published Online March 13, 2013 http://dx.doi.org/10.1016/S1470-2045(13)70045-7

See Comment page 270

*Contributed equally

Impact Genetics and the Toronto Western Hospital Research Institute, University Health Network (D E Rushlow BSc, N L Prigoda-Lee MSc, Prof B L Gallie MD); **Campbell Family Cancer Research Institute, Princess Margaret Cancer Centre, University Health Network** (S Yee MSc, S Pajovic PhD, B L Thériault PhD, C Spencer BSc, C Massey MSc, Prof B L Gallie); **Informatics and Biocomputing Platform, Ontario Institute for Cancer Research** (R Pang MA, P C Boutros PhD); **Department of Hematology/Oncology, Hospital for Sick Children** (H Dimaras PhD); **Department of Ophthalmology and Visual Science, Hospital for Sick Children** (H Dimaras, Prof B L Gallie); **Department of Pathology, Hospital for Sick Children** (W Halliday MD); **Departments of Molecular Genetics and Ophthalmology, University of Toronto** (S Yee, Prof B L Gallie); **Department of Medical Biophysics, University of Toronto** (E Zacksenhaus PhD, Prof B L Gallie); **Department of Pathobiology and Lab Medicine, University of Toronto** (W Halliday); **and Toronto General Research Institute, University Health Network** (Z Jiang BSc, E Zacksenhaus); **Toronto, ON, Canada; Departments of Clinical Genetics, Ophthalmology, and Pediatric Oncology/Hematology, VU University Medical Center Amsterdam, Amsterdam, Netherlands** (B M Mol MSc, A C Moll MD, J C Dorsman PhD); **British Columbia Cancer**

Research Centre and Departments of Ophthalmology and Pathology and Laboratory Medicine, University of British Columbia, Vancouver, BC, Canada (J Y Kennett MSc, K Paton MD, Prof W L Lam PhD); **Eugene and Marilyn Glick Eye Institute, Departments of Ophthalmology, Biochemistry and Molecular Biology, Indiana University School of Medicine Indianapolis, IN, USA** (T W Corson PhD); **University of Alberta, Cross Cancer Institute, Edmonton, AB, Canada** (Prof R Godbout PhD); **Service de Génétique Oncologique, Institut Curie and Université Paris Descartes, Paris, France** (C Houdayer PhD); **Department of Molecular Pathology, Canterbury Health Laboratories, Christchurch, New Zealand** (A Raizis PhD); **and Institut für Humangenetik, Universitätsklinikum, Essen, Germany** (Prof D Lohmann MD)

Correspondence to:
Prof Brenda L Gallie, Campbell Family Cancer Research Institute, Princess Margaret Cancer Centre, University Health Network, Toronto, ON, Canada M5G 1M9
brenda@gallie.ca

See Online for appendix

Service de Génétique Oncologique, Paris, France; Canterbury Health Laboratories, Christchurch, New Zealand; and VU University Medical Center Department of Clinical Genetics, Amsterdam, Netherlands. We obtained tissue samples and clinical data for identification of *RB1* mutations from children in clinical care at these laboratories, and their families. Every laboratory contributed both local and international families. We obtained research ethics board approval to use deidentified data and tissues for clinical analyses, which are on file at every participating site. Although not required, patients from Toronto and Essen provided written informed consent.

Procedures

Full details of Methods are provided in the appendix. We used standard-of-care analyses that identify 95% of *RB1* (Genbank accession L11910.1) mutant alleles.[5–7] Assessments included DNA sequencing, quantitative multiplex PCR (QM-PCR) or multiplex ligation-dependent probe amplification (MLPA), and *RB1* promoter-methylation testing (appendix pp 2–3). To ascertain zygosity of $RB1^{+/+}$ tumours, we used intragenic and closely linked *RB1* microsatellite markers and single nucleotide polymorphisms (SNPs). We did either QM-PCR (Toronto) or MLPA or SNP analyses (Amsterdam) to measure genomic copy numbers of five genes known to be commonly altered in $RB1^{-/-}$ retinoblastomas (*KIF14*, *DEK*, *E2F3*, *CDH11*, and *MYCN*). We used sub-megabase resolution array comparative genomic hybridisation (aCGH) or SNP array to assess overall genomic copy numbers and non-tumour cell contamination (appendix p 3).

We placed three primary $RB1^{+/+}MYCN^{A}$ tumours in the same culture conditions that support growth of $RB1^{-/-}$ cell lines, and we developed these into cell lines (appendix p 4). We stained paraffin-embedded sections of retinoblastomas and adjacent normal retinas for full-length RB1 protein (antibodies targeted N-terminal and C-terminal RB1 protein) and MYCN protein.[8] We did western blots on $RB1^{+/+}MYCN^{A}$ and $RB1^{-/-}$ primary tumours and cell lines, control $RB1^{+/+}$ human fetal and adult retina, and lymphoblastoid and neuroblastoma cell lines (appendix pp 3–4). We did western blotting to assess the function of RB1 protein, using phospho-specific anti-RB1 and coimmunoprecipitation of RB1 and its major effector molecule E2F1. We used endpoint reverse transcriptase PCR (RT-PCR) or quantitative real-time PCR to measure expression of *RB1*, *MYCN*, and genes reflecting the proliferative status and retinal derivation of tumours.

	Total retinoblastoma specimens (n)	$RB1^{+/+}$ tumours (%)	$RB1^{+/+}MYCN^{A}$ tumours (%)
Canada	441	7 (1·6%)	5 (1·1%)
Germany	400	12 (3·0%)	4 (1·0%)
France	150	5 (3·3%)	2 (1·3%)
New Zealand	30	2 (6·7%)	1 (3·3%)
Netherlands	47	3 (6·4%)	3 (6·4%)
Total	1068	29 (2·7%)	15 (1·4%)

Table 1: **Frequency of $RB1^{+/+}$ unilateral retinoblastoma at five diagnostic laboratories**

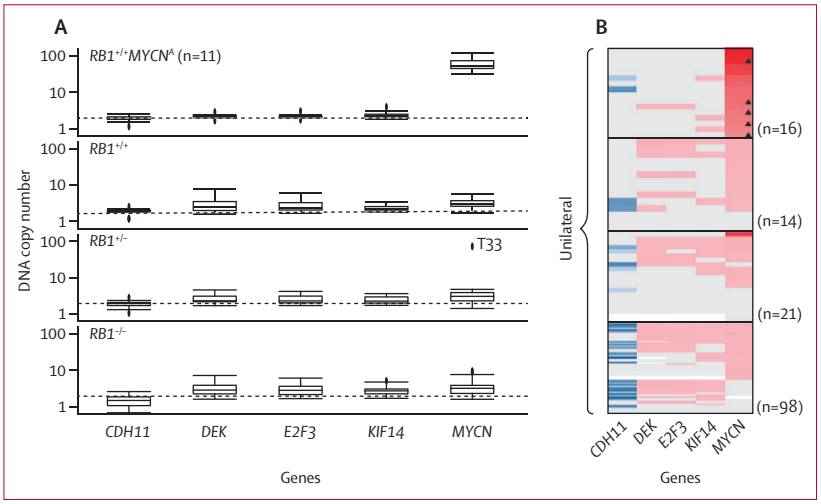

Figure 1: **Copy numbers of genes commonly altered in $RB1^{-/-}$ retinoblastoma**
(A) Box plot of genomic copy numbers ascertained by quantitative multiplex PCR for common genes in unilateral retinoblastoma, grouped by *RB1* mutation status. Specimen T33 is an outlier of the $RB1^{+/-}$ group and shows an $RB1^{+/+}MYCN^{A}$-like profile. Dashed line represents two copies. (B) Heat map for copy number of profile genes. Red=increased copy number. Blue=decreased copy number. Grey=two copies. White=not tested. Black triangles=five $RB1^{+/+}MYCN^{A}$ tumours not included in (A).

Statistical analysis

To assess the likelihood that $RB1^{+/+}$ tumours originated from two undetected *RB1* mutations, we did the χ^2 goodness-of-fit test, using default probabilities of p_1=0·0025 for $RB1^{+/+}$ and p_2=0·9975 for $RB1^{-/-}$ samples (appendix pp 4–5). We established the bimodal distribution of *MYCN* copy number in $RB1^{+/+}$ tumours with a two-tailed *t* test, using Welch's adjustment for heteroscedasticity. We used the statistical program R (version 2.13.2) for these analyses. To compare the proportion of $RB1^{+/+}$ unilateral tumours at every study site and frequencies of specific genomic copy-number changes of tumours with different *RB1* statuses, we used Fisher's exact test (appendix p 13).[9]

We used the *t* test with Welch's adjustment to compare the total number of bp altered per region between $RB1^{+/+}MYCN^{A}$ and $RB1^{-/-}$ tumours (appendix p 5). We processed normalised intensity values with the circular binary segmentation algorithm, with data filtered to identify only high quality (greater than three confirmatory probes) and suitably sized (>25 kbp) regions of clear differential signal relative to normal (|mean–signal| >0·1). We fitted separate terms to groups using a general linear model. We used a contrast matrix to identify the number of differentially abundant probes relative to normal samples with an empirical Bayes moderation of SE and a false-discovery rate adjustment

for multiple testing. We did these analyses with the R statistical program (version 2.11.1), using the DNAcopy (version 1.22.1) and limma (version 3.4.4) packages.

To compare age of diagnosis between groups, we did pairwise comparisons with the Wilcoxon rank-sum test. We estimated the likelihood of children having *RB1*$^{+/+}$*MYCN*^{A} tumours at different ages of diagnosis. We analysed ages at diagnosis versus proportion not yet diagnosed to assess the minimum number of events for tumour initiation (appendix p 5). To ascertain if ages at diagnosis were from a one-hit or two-hit distribution,[1] we estimated the parameter k in the equation ln S=–kT (in which S is the proportion of cases not yet diagnosed and T is age at diagnosis) through a simple linear no-intercept regression analysis. We regressed the empirical values of S on age at diagnosis,[1] assuming an exponential distribution (one-hit), and in the equation ln S=–kT^2, assuming a Weibull distribution with shape parameter of two (two-hit). To compare the relative fit of these data to the two assumptions, we plotted data points for *RB1*$^{-/-}$ and *RB1*$^{+/+}$*MYCN*^{A} cases and the best-fitting curves. We used SAS version 9.3 (TS level 1M1) for analyses of number of events to initiate retinoblastoma.

Role of the funding source

The sponsors of the study had no role in study design, data collection, data analysis, data interpretation, or writing of the report. All authors had full access to all data in the study; the corresponding author (BLG) had final responsibility for the decision to submit for publication.

Results

During clinical work in Toronto, we found seven (1·6%) of 441 unilateral retinoblastoma tumours with no *RB1* mutations, no promoter methylation, and no *RB1* loss of heterozygosity (*RB1*$^{+/+}$). We used QM-PCR to measure, in *RB1*$^{+/+}$ tumours, copy numbers of genes at 6p, 1q, 16q, and 2p that are characteristically gained or lost in *RB1*$^{-/-}$ retinoblastoma tumours.[10] Unexpectedly, five of seven *RB1*$^{+/+}$ tumours showed striking amplification of the *MYCN* oncogene (*MYCN*^{A}). To validate this observation, we collaborated with *RB1* clinical laboratories in Germany, France, and New Zealand. After initial studies, we learnt that the Amsterdam group had independently discovered three *RB1*$^{+/+}$*MYCN*^{A} tumours. We combined our data on 1068 primary unilateral non-familial retinoblastoma tumours after statistical analysis showed that frequencies did not differ by much (p=0·08) between the five laboratories (table 1).

The standard sensitivity for finding the *RB1* mutation in blood samples of bilaterally affected individuals is greater than 95%.[5–7] The probability of finding no *RB1* mutations in a tumour with no *RB1* loss of heterozygosity is equivalent to the probability of missing two independent *RB1* mutations in one sample (0·05×0·05) or 0·25%. By combining our data on 1068 unilateral non-familial tumours, we identified 29 (2·7%) *RB1*$^{+/+}$ tumours, tenfold more than expected (p<0·0001; table 1). Subsequently, a new patient was predicted clinically and pathologically to have an *RB1*$^{+/+}$*MYCN*^{A} tumour (T101), confirmed by *MYCN* copy number; thus, 30 *RB1*$^{+/+}$ retinoblastomas were included in further analyses (appendix p 6).

To characterise copy numbers of genes commonly gained or lost in retinoblastomas,[10] we used QM-PCR (Toronto) or MLPA and SNP (Amsterdam) analyses. *MYCN* copy number was raised in 27 (90%) of 30 *RB1*$^{+/+}$ versus 60 (65%) of 93 *RB1*$^{-/-}$ retinoblastomas (p<0·0001; appendix pp 6–12). None of the 93 *RB1*$^{-/-}$ primary tumours showed more than ten *MYCN* copies. By comparison, 16 (53%) of 30 *RB1*$^{+/+}$ tumours showed high-level *MYCN* amplification (28–121 copies of *MYCN*; p<0·0001; figure 1; appendix pp 6–12, 30). The remaining 14 *RB1*$^{+/+}$ tumours showed between two and ten *MYCN* copies. For ten

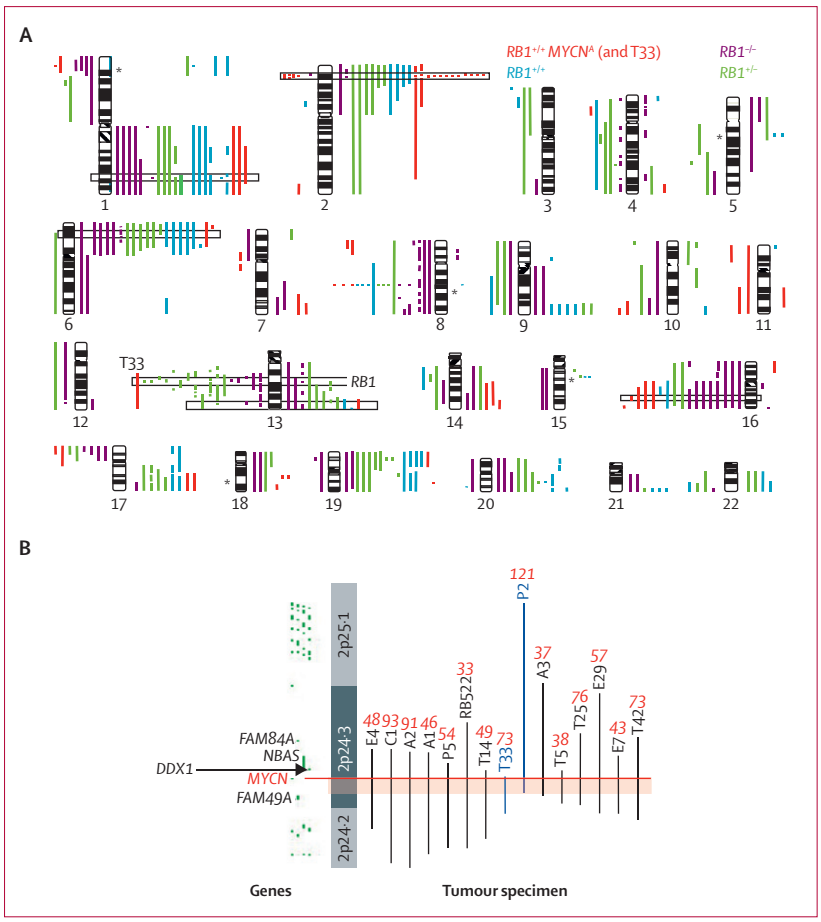

Figure 2: **Genomic copy number alterations**
(A) aCGH of 12 *RB1*$^{+/+}$*MYCN*^{A} (including T33; red), 12 *RB1*$^{+/+}$ (blue), 13 *RB1*$^{+/-}$ (green), and 11 *RB1*$^{-/-}$ (purple) tumours. Gains are shown to the right of the chromosome, losses to the left. Minimum commonly gained or lost regions in *RB1*$^{-/-}$ tumours are boxed. T33 showed a loss of most of 13q. *Normally occurring copy number variations. (B) The minimum amplicon of 513 kbp is defined by two *MYCN*^{A} tumours (pink band). *MYCN* copy number (by QM-PCR) is shown in red italics. aCGH individual probes are denoted as green bars. aCGH=sub-megabase resolution array comparative genomic hybridisation. QM-PCR=quantitative multiplex PCR.

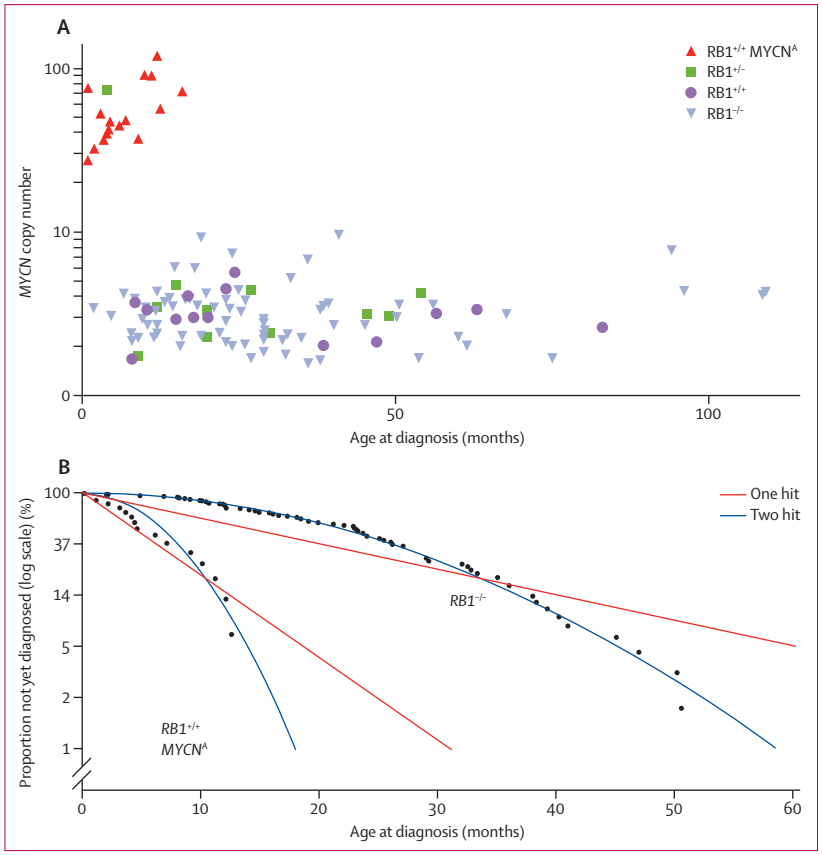

Figure 3: **Clinical features of children with retinoblastomas**
(A) Age at diagnosis of children with retinoblastomas. Children with *RB1*$^{+/+}$*MYCN*^{A} retinoblastomas were significantly younger than those with *RB1*$^{-/-}$ tumours (p<0·0001, Wilcoxon rank sum test). (B) Knudson one-hit and two-hit plots for children with *RB1*$^{-/-}$ or *RB1*$^{+/+}$*MYCN*^{A} tumours, comparing proportion not yet diagnosed with age at diagnosis, using birth as a surrogate for initiation. Scatterplot does not distinguish children of identical ages.

children with *RB1*$^{+/+}$*MYCN*^{A} tumours, DNA from available blood samples showed two *MYCN* copies.

The 16 *RB1*$^{+/+}$*MYCN*^{A} tumours showed a lower frequency of copy-number changes in four other genes characteristic of retinoblastoma, compared with *RB1*$^{-/-}$ retinoblastoma: gain of oncogenes *KIF14* (three of 16 [19%] *vs* 55 of 89 [62%]; p=0·002), *DEK* (one of 16 [6%] *vs* 50 of 87 [57%]; p=0·0002), and *E2F3* (one of 16 [6%] *vs* 52 of 90 [58%]; p=0·0002); and loss of tumour-suppressor gene *CDH11* (two of 16 [13%] *vs* 50 of 90 [56%]; p=0·002; figure 1; appendix pp 6–13). SNP analysis indicated that the level of non-tumour cell contamination in *RB1*$^{+/+}$*MYCN*^{A} tumours was low and similar to *RB1*$^{-/-}$ tumours (appendix p 3).

To probe for other genomic gains or losses, we studied DNA from 48 unilateral retinoblastomas by aCGH[11] (11 *RB1*$^{+/+}$*MYCN*^{A}, 12 *RB1*$^{+/+}$, 14 *RB1*$^{-/-}$, and 11 *RB1*$^{+/-}$ in samples from Canada, Germany, France, and New Zealand) and three *RB1*$^{+/+}$*MYCN*^{A} tumours by SNP analysis (Netherlands; figure 2A; appendix pp 6–12, 14–28, 33). None of the *RB1*$^{+/+}$*MYCN*^{A} retinoblastomas showed any evidence of copy-number changes or translocations[12] at the *RB1* locus. Except for *MYCN* copy number, aCGH (figure 2A) confirmed a reduced frequency in *RB1*$^{+/+}$*MYCN*^{A} retinoblastomas of the specific genomic copy-number changes characteristic of *RB1*$^{-/-}$ retinoblastomas (figure 1; appendix p 13).[10] Also, *RB1*$^{+/+}$*MYCN*^{A} retinoblastomas showed significantly fewer altered bp and aCGH clones overall than did *RB1*$^{-/-}$ retinoblastomas (p=0·033; figure 2A; appendix pp 31, 14–28).

We used aCGH[11] or SNP analysis[3] to study *MYCN* amplifications in 14 *RB1*$^{+/+}$*MYCN*^{A} retinoblastomas, one *RB1*$^{+/-}$ tumour (T33, with 73 *MYCN* copies), and one *RB1*$^{-/-}$ primary tumour (RB381, with 9·2 copies of *MYCN*). *MYCN* amplicons were narrow, spanning 1·1–6·3 Mbp and encompassing *MYCN* (appendix pp 14–28, 32–33). The only copy-number change detected in one *RB1*$^{+/+}$*MYCN*^{A} retinoblastoma (E4) was 48 copies of 2p24·2–24·3, encompassing *MYCN*. The minimum common amplicon defined by retinoblastomas T33 (*RB1*$^{+/-}$) and P2 (*RB1*$^{+/+}$) spanned 513 kbp containing only *MYCN* (figure 2B). *RB1*$^{+/+}$*MYCN*^{A} retinoblastomas T5 and P2 also defined a minimal common amplicon including only *MYCN*. Of the 35 remaining unilateral tumours tested by aCGH (ten *RB1*$^{-/-}$, 13 *RB1*$^{+/+}$, and 12 *RB1*$^{+/+}$), 24 showed no gain or loss at *MYCN*, and 11 had moderate gain spanning a broad region of at least 28 Mbp of chromosome 2p, too large to meet the definition of amplification.[13]

Three of 14 *RB1*$^{+/+}$*MYCN*^{A} tumours showed 17q21·3-qter or 17q24·3-qter gain; two showed 11q loss. Both regions are commonly altered in neuroblastoma,[14,15] but changes are rare in *RB1*$^{-/-}$ retinoblastoma.[16,17] Other changes in *RB1*$^{+/+}$*MYCN*^{A} retinoblastomas not typically seen in *RB1*$^{-/-}$ retinoblastoma were gains at 14q and 18q and losses at 11p (figure 2A; appendix pp 14–20, 33).

Retinoblastoma T33 (*RB1*$^{+/-}$) showed high-level *MYCN* amplification and loss of one copy of most of 13q, including *RB1*; we suspect that amplification of *MYCN* initiated proliferation, followed by 13q deletion. Since T33 showed several characteristics of *RB1*$^{+/+}$*MYCN*^{A} tumours, we included T33 with *MYCN*^{A} retinoblastomas in clinical analyses (figure 2, figure 3A; appendix pp 32, 34).

RB1$^{+/+}$*MYCN*^{A} retinoblastomas and retinal cell types (ganglion cells, specific inner nuclear cells, and cone photoreceptors)[18] expressed functional RB1 protein and showed nuclear staining for C-terminal (figure 4A; appendix p 34) and N-terminal (data not shown) epitopes, whereas *RB1*$^{-/-}$ and *RB1*$^{+/-}$ tumours were negative or stained weakly, depending on their *RB1* mutations. Western blots and immunoprecipitation in three *RB1*$^{+/+}$*MYCN*^{A} cell lines (A3, RB522, and T101) derived from *RB1*$^{+/+}$*MYCN*^{A} primary retinoblastomas showed functional, nuclear, full-length RB1 protein (appendix pp 34–35), normally hypophosphorylated and hyperphosphorylated (figure 4B; appendix p 35), and bound to E2F1 (figure 4C), which is the major target of RB1 protein and controls the cell cycle.[19] Full-length 2·8 kbp *RB1* transcripts were detected by endpoint and real-time

RT-PCR in three *RB1*$^{+/+}$*MYCN*^{A} primary retinoblastomas for which mRNA was available (appendix pp 29, 36). By contrast, four primary *RB1*$^{-/-}$ retinoblastomas expressed low *RB1* transcript levels relative to fetal and adult retina.

RB1$^{+/+}$*MYCN*^{A} primary retinoblastomas (figure 4A) and three derived cell lines (data not shown) stained strongly for MYCN protein. *MYCN* and *KI67* transcripts (indicative of proliferation) were found at low levels in adult retina, at higher levels in fetal retina and in *RB1*$^{-/-}$ retinoblastomas without *MYCN* amplification, and at very high levels in primary *RB1*$^{+/+}$*MYCN*^{A} retinoblastoma and *RB1*$^{-/-}$ cell lines with *MYCN* amplification (appendix pp 29, 36). *RB1*$^{+/+}$*MYCN*^{A} tumours showed reduced expression of the oncogene *KIF14*,[10] by contrast with healthy fetal retina and *RB1*$^{-/-}$ primary retinoblastomas, which overexpressed *KIF14* (appendix pp 29, 36).

RB1$^{+/+}$*MYCN*^{A} tumours expressed embryonic cell markers consistent with a retinal origin. mRNA of cone cell marker X-arrestin[20] and CRX (a marker of retinal and pineal lineage tumours, which is strongly expressed in *RB1*$^{-/-}$ retinoblastoma but not in neuroblastoma)[21] were expressed in fetal retina, human adult retina, and *RB1*$^{+/+}$*MYCN*^{A} and *RB1*$^{-/-}$ primary retinoblastomas (appendix p 36).

Children with *RB1*$^{+/+}$*MYCN*^{A} retinoblastomas were much younger at diagnosis than were those with unilateral *RB1*$^{-/-}$ retinoblastomas. Median age at diagnosis of 17 children with *RB1*$^{+/+}$*MYCN*^{A} tumours (n=16) and *RB1*$^{+/-}$*MYCN*^{A} (T33; n=1) was 4·5 months (IQR 3·5–10), which differed significantly from that for 79 children with unilateral sporadic *RB1*$^{-/-}$ tumours (24 months [15–37]; p<0·0001) and 14 children with *RB1*$^{+/+}$ retinoblastomas (21·5 months [16–45]; p<0·0001; figure 3A; appendix p 9). Age at diagnosis did not differ between patients with *RB1*$^{-/-}$ and *RB1*$^{+/+}$ tumours without *MYCN* amplification (p=0·94). We estimated that 18% of children diagnosed with non-familial unilateral retinoblastoma at age 6 months or younger will have *RB1*$^{+/+}$*MYCN*^{A} retinoblastoma (appendix p 5).

Analysis of age at diagnosis versus proportion not yet diagnosed led Knudson to propose his two-hit model for initiation of retinoblastoma.[1] Our data for 79 unilaterally affected *RB1*$^{-/-}$ patients accorded with Knudson's model and fit a two-hit curve, representative of two independent mutational events in a tumour-suppressor gene (figure 3B). Similar analysis of *RB1*$^{+/+}$*MYCN*^{A} tumours was inconclusive: although datapoints for 12 children diagnosed before age 10 months approximated the calculated one-hit curve, ages for older children deviated (figure 3B).

RB1$^{+/+}$*MYCN*^{A} tumours had distinctive histological features, comprising undifferentiated cells with large, prominent, multiple nucleoli, and necrosis, apoptosis, and little calcification. These features are similar to those seen in other *MYCN*^{A} embryonic tumours, such as neuroblastoma[22] (figure 5A; appendix p 34). Flexner-Wintersteiner rosettes[23] and nuclear moulding, which are characteristic of prototypic *RB1*$^{-/-}$ retinoblastoma (figure 5B), were absent.

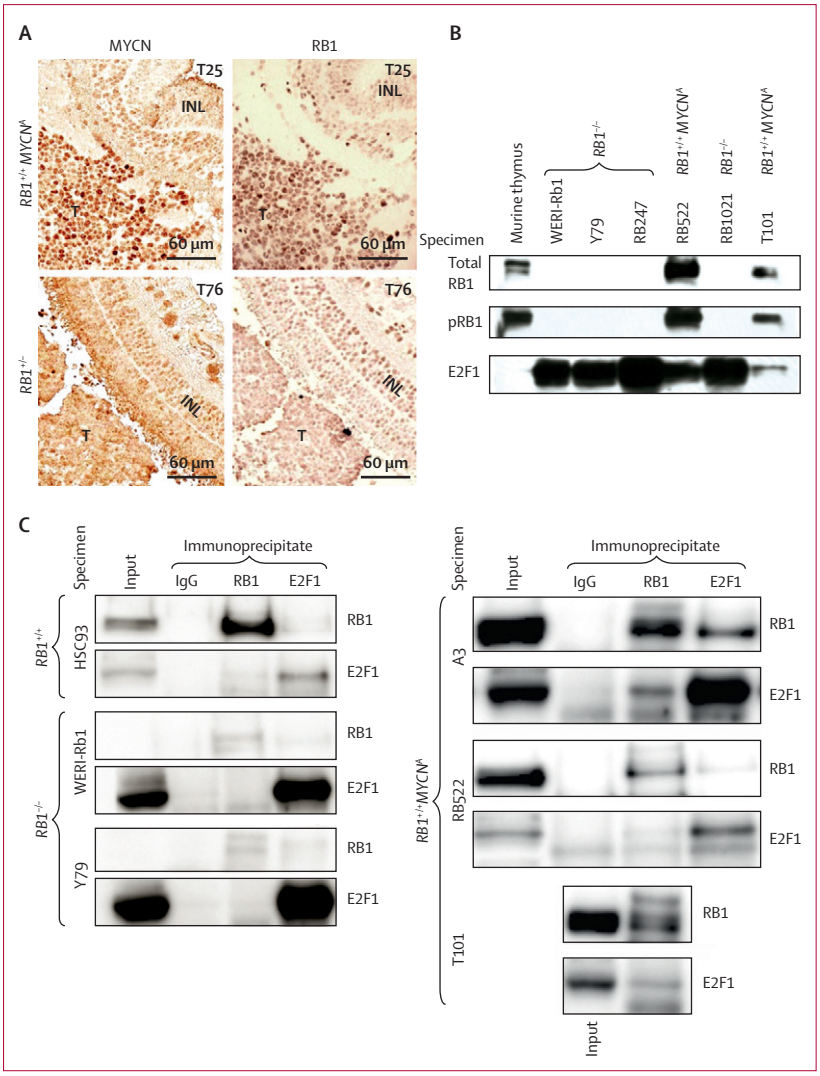

Figure 4: **Expression of *RB1* and *MYCN***

(A) Staining of adjacent retinal tissue and *RB1*$^{+/+}$*MYCN*^{A} or *RB1* mutant retinoblastoma for MYCN protein and RB1 protein (C-terminus antibody). T=tumour. INL=inner nuclear layer retina. (B) Western blots with anti-RB1 that recognises both hypophosphorylated and hyperphosphorylated RB1 protein (total RB1), phospho-RB1 (Ser795) antibody (pRB1), and anti-E2F1. (C) Cell lysates immunoprecipitated with antibodies against mouse IgG (negative control), RB1 protein, and E2F1, and western blots done with antibodies to RB1 and E2F.

Clinically, *RB1*$^{+/+}$*MYCN*^{A} retinoblastomas were large and invasive, in view of the young age of affected children (figure 5C; appendix p 37). One *RB1*$^{+/+}$*MYCN*^{A} retinoblastoma had already invaded the optic nerve past the cribriform plate at age 11 months, a feature of aggressive disease.[24,25] However, with follow-up of 2–25 years, the children with *RB1*$^{+/+}$*MYCN*^{A} tumours had no further evidence of retinoblastoma after removal of their affected eye and none developed retinoblastoma in their other eye.

Discussion

Knudson's analysis of retinoblastoma was fundamental to the idea that normal genes suppress cancer[1] and led to identification of the *RB1* tumour-suppressor gene,[2]

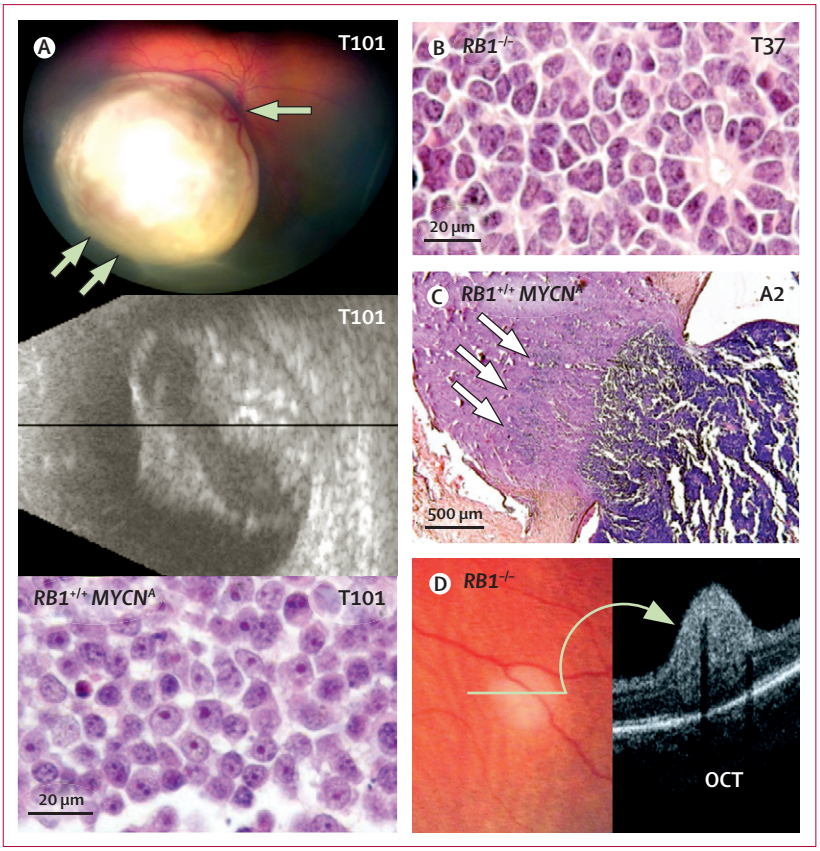

Figure 5: **Clinical features of retinoblastomas**
(A) Fundus image (upper panel) of an *RB1*$^{+/+}$*MYCN*^{A} unilateral tumour (T101), extending from optic nerve (single arrow) to anterior border of retina (double arrows) in a 4-month-old child with characteristic calcification on ultrasound (middle panel) and round nuclei with prominent large multiple nucleoli on histopathology (lower panel). (B) *RB1*$^{-/-}$ tumour (T37) showing classic Flexner-Wintersteiner rosettes and nuclear moulding (haemoxylin and eosin staining). (C) *RB1*$^{+/+}$*MYCN*^{A} retinoblastoma in an 11-month-old child (A2) with extraocular extension into the optic nerve (triple arrows; haemoxylin and eosin staining). (D) 3·5-month-old child with a small, heritable, *RB1*$^{-/-}$ retinoblastoma present in the inner nuclear layer of the retina on optical coherence tomography (OCT).

mutation of which is widely assumed to initiate all retinoblastoma (panel). In this report, we have described a previously unrecognised form of retinoblastoma that has no evidence of *RB1* mutations, displays functional protein, and is probably initiated by amplification of the *MYCN* oncogene.

Of 1068 unilateral non-familial retinoblastomas, we identified a distinct *RB1*$^{+/+}$*MYCN*^{A} subtype that constituted 1·4% of the sample (n=15). At least two previously described tumours might also be *RB1*$^{+/+}$*MYCN*^{A} retinoblastomas,[26] although *RB1* genetic status was not defined. Despite the low frequency of *RB1*$^{+/+}$*MYCN*^{A} retinoblastoma, this tumour subtype was discovered and characterised independently in two laboratories (Toronto and Amsterdam), using different cohorts and technologies. Statistical analyses show that although rare, *RB1*$^{+/+}$*MYCN*^{A} retinoblastomas affect an important subset of patients.

We also identified 14 *RB1*$^{+/+}$ retinoblastomas without *MYCN* amplification. aCGH showed genomic gains and losses that were distinct from either *RB1*$^{-/-}$ or *RB1*$^{+/+}$*MYCN*^{A} retinoblastomas, but we did not have enough *RB1*$^{+/+}$ tumour samples for gene expression or protein studies. In particular, these *RB1*$^{+/+}$ retinoblastomas showed frequent gain of 19p and q, 17p and q, 2p, and the telomeric end of 9q. The *RB1*$^{+/+}$ group seems heterogeneous and merits further study.

Our work highlights how molecular diagnostics can identify novel malignant diseases that elude histopathological recognition. Although *RB1*$^{+/+}$*MYCN*^{A} retinoblastomas have not been recognised previously as a distinct subtype, they resemble large nucleolar neuroblastomas with *MYCN* amplification and poor outcome.[22] Similar to *MYCN*-amplified neuroblastomas,[15] *RB1*$^{+/+}$*MYCN*^{A} tumours have less complex alterations of genomic copy number than do tumours without *MYCN* amplification, suggesting that *MYCN*^{A} could be the important driver of malignancy. However, the early age of diagnosis of *RB1*$^{+/+}$*MYCN*^{A} tumours allows less time to accumulate genomic alterations. Although whole-genome sequencing has suggested that point mutations (other than in the *RB1* gene) are few in *RB1*$^{-/-}$ retinoblastoma,[27] loss of *RB1* induces mitotic changes and lagging chromosomes,[28] leading to genomic instability. Loss of *RB1* in retinoblastoma and premalignant retinoma[8,17] is associated with specific changes in DNA copy number, which are less frequent in *RB1*$^{+/+}$*MYCN*^{A} retinoblastomas.

Are *RB1*$^{+/+}$*MYCN*^{A} tumours truly retinoblastomas? These malignant subtypes arise in and express markers of embryonic retina, meeting the definition of retinoblastoma as a blast-cell tumour arising from the retina.[20,21,29] We showed intact *RB1* genes in primary *RB1*$^{+/+}$*MYCN*^{A} retinoblastomas with strong nuclear RB1 antibody staining. Three *RB1*$^{+/+}$*MYCN*^{A} cell lines expressed full-length *RB1* mRNA and inactive hyperphosphorylated and active hypophosphorylated RB1 protein that coimmunoprecipitated with E2F1, indicating normal functional RB1 protein.[19] The possibility that non-malignant cell contamination could be masking *RB1* mutations in *RB1*$^{+/+}$*MYCN*^{A} tumours is ruled out because three *RB1*$^{+/+}$*MYCN*^{A} cell lines grew rapidly from the primary tumours, unlike *RB1*$^{-/-}$ retinoblastoma, and maintained the *RB1*$^{+/+}$*MYCN*^{A} genotype of the primary tumours.

Although next-generation DNA sequencing is a powerful discovery technique, its clinical application has not yet achieved sensitivity to match *RB1* mutation detection technologies. If an *RB1* mutation were identified by the next-generation enhanced read depth approach, that variant would represent convergent evolution to knockout RB1 protein with cancer progression, common in many cancers, rather than an initiating *RB1* mutation. Based on the cell-line genotypes, the *MYCN* amplification would still be the event common to all cells and, thereby, the probable initiating event.

The very early presentation of *RB1*$^{+/+}$*MYCN*^{A} retinoblastomas, absence of *RB1* mutations, functional RB1 protein, and high *MYCN* amplification in a genome with a

fairly stable copy number suggests that these tumours arise by somatic *MYCN* oncogene amplification in a retinal progenitor cell. This idea is supported by the finding of one *RB1*$^{+/+}$*MYCN*^{A} tumour in which *MYCN* amplification was the only identified genomic copy-number change. *RB1*$^{+/+}$*MYCN*^{A} retinoblastomas are already large in very young children so they probably are initiated earlier in retinal development than are *RB1*$^{-/-}$ retinoblastomas. In children with an *RB1* mutation of equivalent age, tumours are usually much smaller (figure 5D). The method by which *MYCN* amplification is initiated, and whether *MYCN* amplification alone is sufficient to initiate retinoblastoma, remains to be shown formally.

In retinal development, the MYCN protein can support cell division without activation of the E2F family of transcription factors; presumably, unregulated *MYCN* expression associated with high-level gene amplification in *RB1*$^{+/+}$*MYCN*^{A} tumours promotes cell division by indirect inactivation of RB1 protein.[30] The relative genomic stability of *RB1*$^{+/+}$*MYCN*^{A} retinoblastomas could result in less resistance to treatment, which is seen in *RB1*$^{-/-}$ retinoblastoma associated with progressive genomic rearrangements. Our preliminary *MYCN* knock-down experiments resulted in rapid death of *RB1*$^{+/+}$*MYCN*^{A} cell lines (data not shown). We predict that, worldwide, infants younger than 1 year[24] with extraocular retinoblastoma could have *RB1*$^{+/+}$*MYCN*^{A} tumours and might benefit from anti-MYCN treatment.[31] This idea accords with an anecdotal observation by one of us (BLG) during review of retinoblastoma pathology slides in Kenya, of *RB1*$^{+/+}$*MYCN*^{A} histological findings in an orbital recurrence, later confirmed to have 40 *MYCN* copies.

The young age at diagnosis of unilateral retinoblastoma is interpreted frequently as an indication of heritable disease and is cited as a reason to try to cure the cancer without enucleation. However, attempts to salvage an eye with a large *RB1*$^{+/+}$*MYCN*^{A} retinoblastoma could be dangerous. In our study, no further retinoblastoma was identified after prompt removal of the unilateral affected eye, with no adverse outcomes. The young patients with *RB1*$^{+/+}$*MYCN*^{A} tumours in our study had large aggressive tumours, including invasion into the optic nerve (figure 5C). At similar young ages, usual hereditary *RB1*$^{-/-}$ tumours are much smaller, detected only by active surveillance (figure 5D). Although we predict that 18% of children diagnosed with non-familial unilateral retinoblastoma at age 6 months or younger will have *RB1*$^{+/+}$*MYCN*^{A} retinoblastoma (appendix p 5), if tumour size is also considered, *RB1*$^{+/+}$*MYCN*^{A} tumours might be clinically predictable, facilitating prompt removal of these eyes with good outcomes for children.

Standard care for unilateral non-familial retinoblastoma is identification of the *RB1* mutant alleles in the tumour and examination of blood to ascertain whether either mutant allele is germline. When no *RB1* mutation is detected in a retinoblastoma tumour, establishing the *MYCN* copy number could assist ongoing care. Diagnosis of *RB1*$^{+/+}$*MYCN*^{A} retinoblastoma strongly suggests non-hereditary disease, with normal population risks for retinoblastomas in the other eye and for other cancers throughout life, and no familial risks.

Our findings challenge the longstanding dogma that all retinoblastomas are initiated by *RB1* gene mutations. *RB1*$^{+/+}$*MYCN*^{A} retinoblastoma differs from classic retinoblastoma in terms of both genetics and clinical characteristics (table 2), with immediate relevance to patients.

Panel: Research in context

Systematic review

We systematically searched PubMed with the terms: "retinoblastoma", "initiation", and "genetics"; "retinoblastoma tumour genetics"; "retinoblastoma development"; and "retinoblastoma initiation". We reviewed retrieved publications with a main focus on genetic initiation and development of human retinoblastoma. We identified no data to challenge Knudson's 1971 conclusion that two rate-limiting events,[1] later shown to be loss of both *RB1* gene alleles,[2–5,7] are essential, but not necessarily sufficient, for development of retinoblastoma. We found no data to suggest other forms of retinoblastoma.

Interpretation

With our collaborative studies, we identified a previously unrecognised disease: retinoblastoma with normal *RB1* genes, apparently driven by *MYCN* oncogene amplification. This new form of retinoblastoma has immediate clinical implications for patients. *RB1*$^{+/+}$*MYCN*^{A} retinoblastomas are diagnosed by molecular study of the tumour after removal of the eye of very young children with unilateral non-familial disease. Children with *RB1*$^{+/+}$*MYCN*^{A} retinoblastoma and their relatives are predicted to be at normal population risk for other cancers. Attempts to salvage the eye on the assumption of heritable disease in young children could incur high treatment morbidity and failure to cure these aggressive oncogene-driven retinoblastomas.

	Classic *RB1*$^{-/-}$	Novel *RB1*$^{+/+}$*MYCN*^{A}
RB1 status	–/–	+/+
RB1 protein expression	Rare	Full-length, nuclear, phosphorylated, binds E2F1
Specific and general genomic gains and losses	Common	Uncommon
MYCN copy number	2–9 copies, wide region	28–121 copies, narrow amplicon
MYCN mRNA expression	Moderate	High
Histological characteristics	Rosettes	Multiple nucleoli and blast cells
Median (IQR) age at diagnosis (months)	24 (15–37)	4·5 (3·5–10)

Table 2: **Differences between classic *RB1*$^{-/-}$ tumours and novel *RB1*$^{+/+}$*MYCN*^{A} unilateral non-familial retinoblastoma**

Our findings challenge the longstanding dogma that all retinoblastomas are initiated by *RB1* gene mutations. *RB1*$^{+/+}$*MYCN*^{A} retinoblastoma differs from classic retinoblastoma in terms of both genetics and clinical characteristics (table 2), with immediate relevance to patients.

Contributors

DER recognised the initial connection between *MYCN* amplification and *RB1* mutation status, did the literature search and QM-PCR analysis, supervised *RB1* mutation analysis, coordinated collaborations with the other sites, and made a major contribution to preparation of the report. BMM recognised the *RB1* and *MYCN* mutation status of the Amsterdam samples and did MLPA and SNP array analysis, western blots, and coimmunoprecipitation. JYK did aCGH and analysed aCGH data. SY analysed aCGH data and the *MYCN*^{A} alignment and did immunohistochemistry and RT-PCR. SP did the literature search and RT-PCR and immunohistochemistry. BLT did the literature search and RNA expression studies. NLP-L did the literature search and statistical analyses, grew cell lines, and contributed to preparation of figures and the report. CS did immunohistochemistry. HD and TWC did the

literature search, assisted with data analysis and ideas for the discussion, and contributed to preparation of figures and the report. RP did statistical and bioinformatic analyses on aCGH data. CM did statistical analyses. RG discovered and characterised the first tumour with *MYCN* amplification and normal RB1 protein (RB522; now *RB1*$^{+/+}$*MYCN*^{A}) and provided the cell line and western blot showing multiple bands of RB1 protein. ZJ and EZ did western blots specific to phosphorylated RB1 protein. KP and ACM provided and interpreted clinical data and images. CH and AR did *RB1* mutation analysis and provided clinical data. WH recognised and characterised the histological features of *RB1*$^{+/+}$*MYCN*^{A} retinoblastomas and prepared digital images for publication. WLL supervised JYK and the aCGH experiments. PCB did detailed analyses of aCGH data and statistical analyses throughout the project and supervised RP. DL did the literature search and *RB1* mutation analysis and contributed to preparation of figures and development of ideas. JCD coordinated the Amsterdam study, recognised the *RB1* and *MYCN* mutation status of the Amsterdam samples, and supervised BMM. BLG supervised the overall study, did the literature search, provided guidance on all parts of the project, and contributed to preparation of figures and the report. All authors contributed ideas and helped to write the report.

Conflicts of interest

BLG was part-owner of Solutions by Sequence and was a board member of Retinoblastoma Solutions (now Impact Genetics, of which BLG is medical director). All other authors declare that they have no conflicts of interest.

Acknowledgments

We thank the sponsors of the study: the National Cancer Institute–National Institutes of Health (grant 5R01CA118830-05 [BLG]); Canadian Institutes for Health Research (grants MOP-86731, MOP-77903, and MOP-110949 [WLL], and MOP-77710 [EZ]); the Canadian Retinoblastoma Society; Hyland Foundation; Toronto Netralaya and Doctors Lions Clubs; the Alcon Research Institute; the Ontario Ministry of Health and Long Term Care; Retinoblastoma Solutions and Solutions by Sequence (now Impact Genetics); the German Research Foundation (grant Lo 530/6-2); UK-Essen; Avanti-STR (JCD, J Cloos, and ACM); KiKa (JCD, H te Riele, J Cloos, ACM); VU University Medical Center; Ontario Institute for Cancer Research and the Government of Ontario (PCB); CCA/V-ICI/Avanti-STR (BMM); the Vision Science Research Program of the University Health Network and the University of Toronto (SY); and Queen's University School of Medicine (Great West Life Studentship [RP]). We thank: Irsan Kooi (VU University Medical Center) for assessment of normal-cell contamination by SNP data; Leslie MacKeen for the collage of RetCam images in figure 3B; Valerie White (University of British Columbia) for clinical and pathological details and images; Cynthia Vandenhoven for clinical images in figure 5; members of the VU University Medical Center/the Netherlands Cancer Institute, Institut Curie, Institut für Humangenetik, Toronto retinoblastoma teams, and other colleagues for useful discussions; and the children and families who donated tissues for these studies.

References

1 Knudson AG. Mutation and cancer: statistical study of retinoblastoma. *Proc Natl Acad Sci USA* 1971; **68:** 820–23.

2 Friend SH, Bernards R, Rogelj S, et al. A human DNA segment with properties of the gene that predisposes to retinoblastoma and osteosarcoma. *Nature* 1986; **323:** 643–46.

3 Cavenee WK, Hansen MF, Nordenskjold M, et al. Genetic origin of mutations predisposing to retinoblastoma. *Science* 1985; **228:** 501–03.

4 Lohmann DR, Gallie BL. Retinoblastoma: revisiting the model prototype of inherited cancer. *Am J Med Genet* 2004; **129C:** 23–28.

5 Rushlow D, Piovesan B, Zhang K, et al. Detection of mosaic RB1 mutations in families with retinoblastoma. *Hum Mutat* 2009; **30:** 842–51.

6 Lohmann D, Gallie B, Dommering C, Gauthier-Villars M. Clinical utility gene card for: retinoblastoma. *Eur J Hum Genet* 2010; published online Dec 8. DOI:10.1038/ejhg.2010.200.

7 Houdayer C, Gauthier-Villars M, Lauge A, et al. Comprehensive screening for constitutional RB1 mutations by DHPLC and QMPSF. *Hum Mutat* 2004; **23:** 193–202.

8 Dimaras H, Khetan V, Halliday W, et al. Loss of RB1 induces non-proliferative retinoma: increasing genomic instability correlates with progression to retinoblastoma. *Hum Mol Genet* 2008; **17:** 1363–72.

9 Lowry R. For a 2x2 contingency table. 2013. http://www.vassarstats.net/tab2x2.html (accessed Feb 11, 2013).

10 Corson TW, Gallie BL. One hit, two hits, three hits, more? Genomic changes in the development of retinoblastoma. *Genes Chromosomes Cancer* 2007; **46:** 617–34.

11 Ishkanian AS, Malloff CA, Watson SK, et al. A tiling resolution DNA microarray with complete coverage of the human genome. *Nat Genet* 2004; **36:** 299–303.

12 Watson SK, deLeeuw RJ, Horsman DE, Squire JA, Lam WL. Cytogenetically balanced translocations are associated with focal copy number alterations. *Hum Genet* 2007; **120:** 795–805.

13 Myllykangas S, Bohling T, Knuutila S. Specificity, selection and significance of gene amplifications in cancer. *Semin Cancer Biol* 2007; **17:** 42–55.

14 O'Neill S, Ekstrom L, Lastowska M, et al. MYCN amplification and 17q in neuroblastoma: evidence for structural association. *Genes Chromosomes Cancer* 2001; **30:** 87–90.

15 Mosse YP, Diskin SJ, Wasserman N, et al. Neuroblastomas have distinct genomic DNA profiles that predict clinical phenotype and regional gene expression. *Genes Chromosomes Cancer* 2007; **46:** 936–49.

16 Chen D, Gallie BL, Squire JA. Minimal regions of chromosomal imbalance in retinoblastoma detected by comparative genomic hybridization. *Cancer Genet Cytogenet* 2001; **129:** 57–63.

17 Sampieri K, Amenduni M, Papa FT, et al. Array comparative genomic hybridization in retinoma and retinoblastoma tissues. *Cancer Sci* 2009; **100:** 465–71.

18 Spencer C, Pajovic S, Devlin H, Dinh QD, Corson TW, Gallie BL. Distinct patterns of expression of the RB gene family in mouse and human retina. *Gene Expr Patterns* 2005; **5:** 687–94.

19 Templeton DJ, Park SH, Lanier L, Weinberg RA. Nonfunctional mutants of the retinoblastoma protein are characterized by defects in phosphorylation, viral oncoprotein association, and nuclear tethering. *Proc Natl Acad Sci USA* 1991; **88:** 3033–37.

20 Murakami A, Yajima T, Sakuma H, McLaren MJ, Inana G. X-arrestin: a new retinal arrestin mapping to the X chromosome. *FEBS Lett* 1993; **334:** 203–09.

21 Terry J, Calicchio ML, Rodriguez-Galindo C, Perez-Atayde AR. Immunohistochemical expression of CRX in extracranial malignant small round cell tumors. *Am J Surg Pathol* 2012; **36:** 1165–69.

22 Tornoczky T, Semjen D, Shimada H, Ambros IM. Pathology of peripheral neuroblastic tumors: significance of prominent nucleoli in undifferentiated/poorly differentiated neuroblastoma. *Pathol Oncol Res* 2007; **13:** 269–75.

23 Flexner S. A peculiar glioma (neuroepithelioma?) of the retina. *Johns Hopkins Hosp Bull* 1891; **2:** 115.

24 Dimaras H, Kimani K, Dimba EAO, et al. Retinoblastoma. *Lancet* 2012; **379:** 1436–46.

25 Chantada GL, Casco F, Fandino AC, et al. Outcome of patients with retinoblastoma and postlaminar optic nerve invasion. *Ophthalmology* 2007; **114:** 2083–89.

26 Lillington DM, Goff LK, Kingston JE, et al. High level amplification of N-MYC is not associated with adverse histology or outcome in primary retinoblastoma tumours. *Br J Cancer* 2002; **87:** 779–82.

27 Zhang J, Benavente CA, McEvoy J, et al. A novel retinoblastoma therapy from genomic and epigenetic analyses. *Nature* 2012; **481:** 329–34.

28 Manning AL, Longworth MS, Dyson NJ. Loss of pRB causes centromere dysfunction and chromosomal instability. *Genes Dev* 2010; **24:** 1364–76.

29 Kobayashi M, Takezawa S, Hara K, et al. Identification of a photoreceptor cell-specific nuclear receptor. *Proc Natl Acad Sci USA* 1999; **96:** 4814–19.

30 Chen D, Pacal M, Wenzel P, Knoepfler PS, Leone G, Bremner R. Division and apoptosis of E2f-deficient retinal progenitors. *Nature* 2009; **462:** 925–29.

31 Hook KE, Garza SJ, Lira ME, et al. An integrated genomic approach to identify predictive biomarkers of response to the aurora kinase inhibitor PF-03814735. *Mol Cancer Ther* 2012; **11:** 710–19.